Journal of Engineering and Applied Sciences 14 (Special Issue 5): 8933-8939, 2019
ISSN: 1816-949X

Optimum Standstill Electronic Commutation Process for Encoderless PM Machines

[1]Mazen M. A. Al Ibraheemi and [2]Fatih J. Anayi
[1]Faculty of Engineering, Al Qadisiya University, Iraq
[2]Wolfson Centre for Magnetics, Cardiff University, Cardiff CF24 3AA, U.K

Abstract: This study presents a novel encoderless method to ensure an optimum energising sequence to stator windings of PM machines. The work strategy was achieved through exploiting the machine terminal voltages to obtain an approximate estimation for N-pole position of the rotor permanent magnet, PM. Implementation of the proposed technique based on injection of short duration signals into the machine stator windings and monitoring the corresponding voltage responses at the machine terminals. Then, the responses were employed in dividing the 360 degrees of rotor whole space into domains. A MATLAB model was built to achieve the proposed concept and to define the domain number at which the rotor is halting. Thereby, the optimum standstill excitation sequence for stator windings, commutation process, was defined.

Key words: N-pole position prediction, voltage measurements, rotor domais, permanent magnet machines, encoderless estimation

INTRODUCTION

Permanent magnet, PM, machines has recently gained a leading position in many industrial fields. This comes due to the considerable feature of those machines, such as, low pollution and high reliability. Determining the standstill position of the N-pole of PM has a crucial impact to insure an optimum commutation process and, consequently, safe start-up for these machines. Although the sensor methods have an accurate performance in determining the required positions, they have many drawbacks which lead to increase the trends toward encoderless techniques (Dost and Sourkounis, 2011). Moreover, a soft machine running with a minimum torque ripple and maximum output power can be taken out if the standstill commutation process is accurately achieved (Assegaf *et al*., 2013; Fang *et al*., 2009; Jebai *et al*., 2016; Setty *et al*., 2012).

Accordingly, many efforts were made, since the last two decades, to solve the problem of standstill PM position determining. A scheme was proposed in 1995 to determine the position and speed of rotor shaft of ac machine, including the start-up position. It was done through injection of 3-phase high frequency signal and detecting the position by implementing a demodulation process to exploit the machine magnetic saliency track (Yang, 2014; Zhaobin *et al*., 2014; Pillai *et al*., 2015). Another detection method for PM initial position was introduced by Kim *et al*. (2004) through injection of high frequency carrier signals. A second order Taylor series for the relation between stator current and flux linkage in d-axis rotor reference frame was used to detect the polarity of PM. Wang *et al*. (2009) exploited the considerable amount of magnetic flux linkage produced by the PM to monitor the noticeable change in inductances of rotor reference frame L_d and L_q which should involve information about the zero speed rotor position. A method for rotor position estimation by applying voltage pulses and measuring the peaks of the resulting currents was presented by Moghadam and Tahami, (2012). This method involved an iterative voltage sequence combined with fuzzy logic processing of current responses in order to avoid the uncertainty in values of currents.

Deshpande *et al*. (2012) presented 30° resolution rotor position estimation through measuring the line-to-line back EMF when two windings are supplied with dc voltage. Zhang *et al*. (2005) introduced a technique to detect the polarity of magnet and angle position of rotor at zero speed. This initialization process was achieved by injecting high frequency signal and sequence of current pulses composed of two pulses. Again the saturation in stator iron core was exploited here. Moreover, the injected current should possess a high value enough to produce noticeable change in iron saturation.

The work presented in this study proposes a novel method for optimum startup of permanent magnet machine through creating a relation between voltage responses of the machine windings and rotor position. The study has been organized in five sections as follow: after the introduction, in section I, the theoretical

Corresponding Author: Mazen M. A. Al Ibraheemi, Faculty of Engineering, Al Qadisiya University, Iraq

background is reviewed in section II, then section III introduces the MATLAB model, section IV is assigned for exploring the results and finally section V underscores the conclusions.

THEORY

At standstill, any two, of the three stator windings of a permanent magnet, PM, machine can be excited while the third winding is exploited as a voltage sensor (Iizuka *et al*., 1985). This principle was employed in this study, where three signals, each of a short time duration, were used as an excitation test signals for the series machine windings A-B, A-C and B-C respectively. The voltage drop across each of the excited winding was observed via the third unexcited winding, free machine terminal.

Analysis of PM machine: The mathematical relations for PM machine parameters with voltages, current and air gap flux can described in the rotary reference frame, dq-frame, as follow:

$$\begin{bmatrix} u_{sd} \\ u_{sq} \end{bmatrix} = \begin{bmatrix} R_s & 0 \\ 0 & R_s \end{bmatrix} \begin{bmatrix} i_{sd} \\ i_{sq} \end{bmatrix} + \begin{bmatrix} p & -\omega_r \\ \omega_r & p \end{bmatrix} \begin{bmatrix} \varphi_{sd} \\ \varphi_{sq} \end{bmatrix} \quad (1)$$

where, R_s is the stator winding phase resistance, is the derivative notation, is the rotor speed, are the stator voltages currents in dq-frame and are the air gap flux linkages which are given by:

$$\begin{bmatrix} \varphi_{sd} \\ \varphi_{sq} \end{bmatrix} = \begin{bmatrix} L_s & 0 \\ 0 & L_s \end{bmatrix} \begin{bmatrix} i_{sd} \\ i_{sq} \end{bmatrix} + \begin{bmatrix} \varphi_r \\ 0 \end{bmatrix} \quad (2)$$

where, represent the stator self-phase inductance and the PM flux respectively.

Graphically, those relations can be expressed as shown in the following vector diagram, Fig. 1, together with the stationary reference frame representation, αβ-frame, where θ represents the PM flux direction with respect to position of phase A:

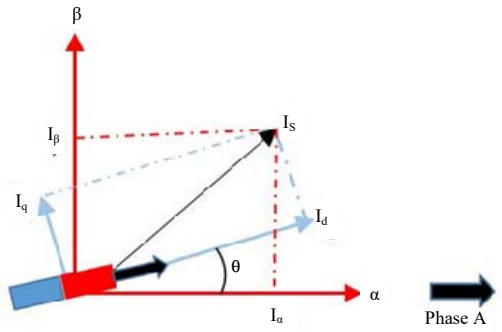

Fig. 1: Vector representations for PM machine variables

At standstill and the voltage equation, equation 1, becomes:

$$\begin{bmatrix} u_{sd} \\ u_{sq} \end{bmatrix} = \begin{bmatrix} R_s & 0 \\ 0 & R_s \end{bmatrix} \begin{bmatrix} i_{sd} \\ i_{sq} \end{bmatrix} + \begin{bmatrix} p & 0 \\ 0 & p \end{bmatrix} \begin{bmatrix} \varphi_{sd} \\ \varphi_{sq} \end{bmatrix} \quad (3)$$

Taking into consideration the magnetic saliency impact of the PM, then the rotor field component, which is perpendicular to direction of stator windings, effects on the self-inductances so that they become variant, L, with rotor position as follow:

$$L = L_{st} \mp L_{max} \cos(\theta) \quad (4)$$

where, refers to the maximum variation in stator inductances, L_A, L_B and L_C due to the PM saliency. Figure 2 gives a MATLAM/SIMULATION view for this concept.

Methodology of PM domain determinations: Figure 3 illustrates applying a low level excitation pulses of a short width at the gate of the switching elements (IGBTs 1 and 6) so as to excite windings A and C. Both IGBTs respond by transiting to ON condition. The responses produce voltage pulses between terminals of windings A and C. The amplitudes of these voltage pulses equal the dc link voltage V_{dc} and their duration equal to that of the applied excitation pulses on the gates of the switching elements. The red route, in this figure, highlights the current flow under the effect of the ON condition transients. In this case, as the terminal of winding C is connected to ground, its voltage drop, V_C, is measured through the free winding B. Mathematically, this action can be described by following equation:

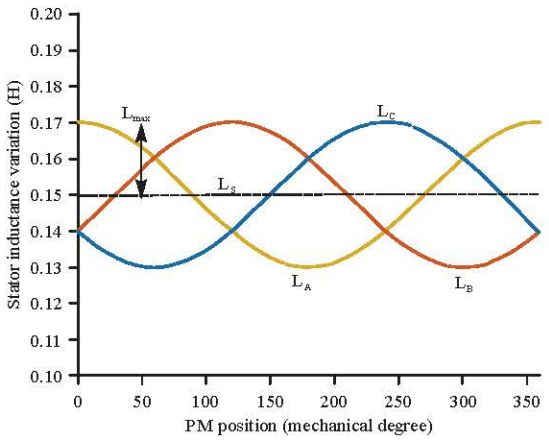

Fig. 2: Modelling stator inductance variations with PM position

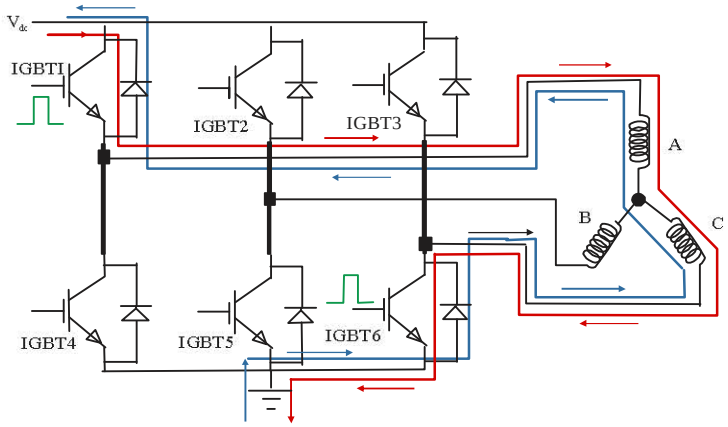

Fig. 3: Injection of pulses in windings A and C

$$V_{dc} = V_A + V_c = i_{dc}\,(R_A+R_C)+(L_A(\theta)+L_C(\theta))\,di_{dc}/dt \quad (5)$$

Under the rapid switching speed caused by applying high frequency injected pulses, the PM machine can be seen as a simple L load. Therefore, the resistive component effect can be ignored comparing to that of the inductive. Moreover, the period of the injected signal should be smaller than the time constant of each of the stator windings. This is to ensure that the signals will not be able to influence the PM to be shifted from the standstill position. Therefore, the variation of the dc bus current will be in a constant rate, k. accordingly, equation 4 can be rewritten as follow:

$$i_{dc} = \frac{V_{dc}}{k*(L_A(\theta)+L_C(\theta))} \quad (6)$$

Consequently, the measured voltage for winding C will be variant with PM position and equal to:

$$V_C(\theta) = V_{dc}\frac{L_C(\theta)}{k*(L_A(\theta)+L_C(\theta))} \quad (7)$$

Directly after absence of the applied pulses, flow of the flyback current starts flowing which is illustrated on the figure by the blue route. In this case, manner of connection of the excited winding is reversed, so the voltage drop across the winding connected to ground, V_A, is measured. Similar to derivation of equation 6, V_A equation can be derived and so for other voltages due to injection of other signals.

Thereby, three voltage responses directly yield from signal injections and three other from the flyback reactions. Comparison results of these voltages are employed to determine the numerical notation for the PM location at the moment of testing. Each numerical notation refers to an angular band within the PM whole space.

MODELLINrG THE COMMUTATION PROCESS

Figure 4 shows details of the MATLAB-SIMULINK model for determining the PM location and accordingly defining the best standstill electronic commutation process.

In this figure, two voltage responses, at different timing, were measured at each of the three machine terminals. They were passed through delay time circuitries, D, to be read simultaneously at the moment of simulation ending period. Therefore, six delay structures, D_1 through D_6, are shown in the figure and they are also shown with their values on Fig. 6. The two voltage responses, at each machine terminal, were magnitudelly compared. So, three binary comparison results, u_1, u_2 and u_3 were obtained. The user function block, f(u), was employed to rewrite the inputs into decimal form using the code '1 2 4 8' as following:

$$f(u) = 1*u_1+2*u_2+4*u_3 \quad (8)$$

Thereby, the output of the f(u) block indicated the sub-domain number at which the N-pole of the PM was located at the moment of simulation. However, indicating the main domain number is not shown in this figure because it needs to magnetic polarity detection method which is currently out of the topic of this work. It may be worth to mention here that the polarity technique works only in case of one pole-pair and it requires more complicated polarity detection technique in case of more than one pole-pairs machine.

Table 1 shows the parameters of the PM synchronous machine which was regarded as a MATLAB-SIMULINK model in the simulation tests to verify the proposed work.

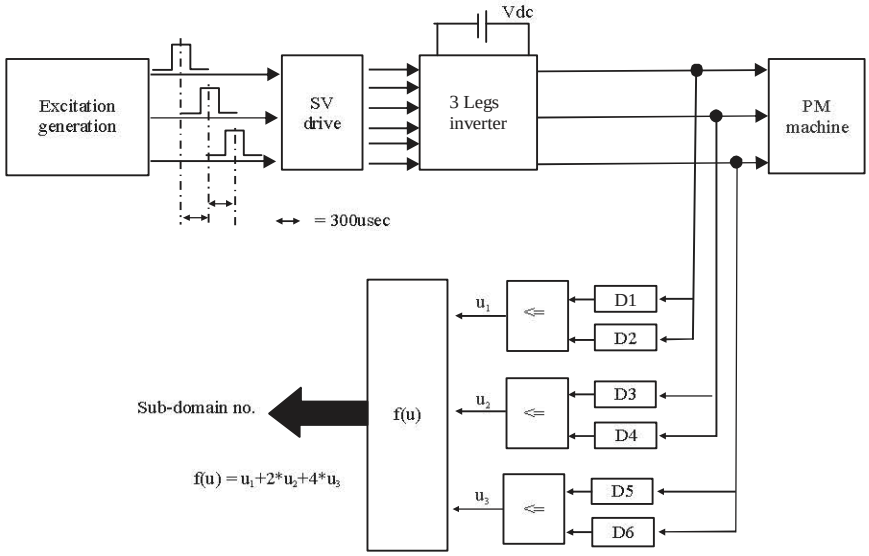

Fig. 4: MATLAB-SIMULINK model for PM position defining

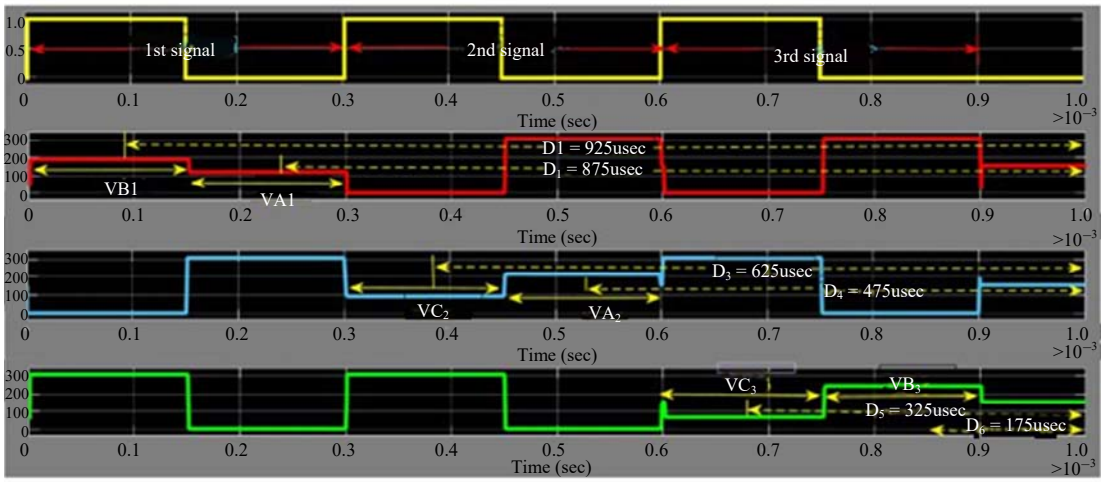

Fig. 5: Resultant voltage responses due to injection of three signals when the PM at 45°

SIMULATION RESULTS

Figure 5 shows the three applied signals and the corresponding responses when the PM was located at 45°, as they were simulated by MATLAM-SIMULINK modelling for a PM machine of one pole-pair. The first injected signal yielded the responses VB1 and VA1 while VC2, VA2, VC3 and VB3 were obtained from the second and third injected signals respectively.

Events of signal injections and voltage response measurements were frequently achieved over the whole spatial angles from 0-360 degrees. Figure 6 shows a graphical representation for those voltage responses.

The simulation results showed that for one pole-pair machine, the complete magnetic cycle of PM divides the whole spatial space into two similar main domains. Whereas, each main domain is further divided into six sub-domains. Moreover, increasing the number of pole-pairs caused corresponding increasing in the main domain divisions and in the frequency of the voltage responses through increasing the magnetic cycles and vice versa. While the sub-domain numbers within each main domain did not change. Table 2 summarises the above results.

From this table, one can deduce the following relations:

$$\text{No. of main domains} = 2 \times \text{No of pole-pairs} \quad (9)$$

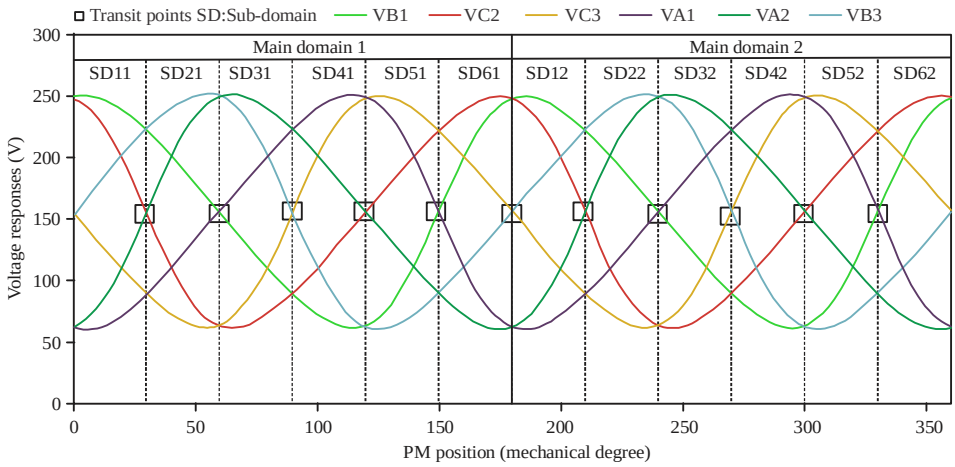

Fig. 6: Six voltage responses over the whole spatial of PM

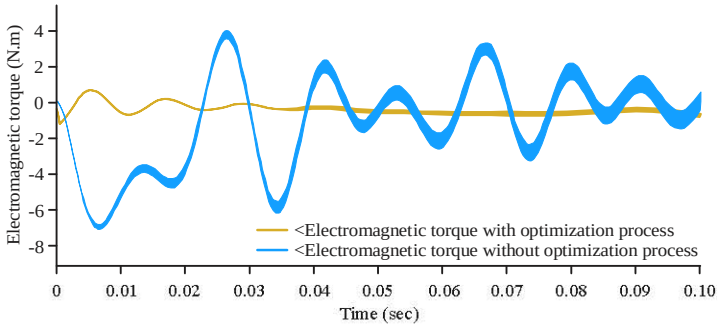

Fig. 7: Start-up electromagnetic torque with and without optimization process

Table 1: Parameters of PM machine under test

Parameters	Values
No. of phases	3
No. of poles	1, 2 or 3
Stator phase resistance	1 Ω
Stator phase inductance	$L_d = 8.5$ $L_q = 17$ (mH)
PM flux	0.28576 V.s
Inertia	0.00027 J (kg,m^2)
DC link voltage	310 V

Table 2: Changes of main and sub domains with no. of pole-pairs

	Main domains		Sub-domains	
No. of pole-pairs	No.	Width	No.	Width
1	2	180°	6	30°
2	4	90°	6	15°
3	6	60°	6	10°

$$\text{Width of sub-domain} = \frac{360}{\text{No.of sub} - \text{domains} \times \text{No.of main domain}} \quad (10)$$

The best standstill commutation prosses with respect to the domain at which the PM is located is summarised in Table 3.

Table 3: Optimum commutation process with main and sub domain numbers

Main domain	Sub-domain	Commutation process	SV domain
1	1	A^+, B^-, C^-	100
1	2	A^+, B^+, C^-	110
1	3	A^-, B^+, C^-	010
1	4	A^-, B^+, C^+	011
1	5	A^+, B^-, C^+	101
1	6	A^-, B^-, C^+	001
2	1	A^-, B^+, C^+	011
2	2	A^-, B^-, C^+	001
2	3	A^+, B^-, C^+	101
2	4	A^+, B^-, C^-	100
2	5	A^-, B^+, C^-	010
2	6	A^+, B^+, C^-	110

For instant, the first state in Table 3 determines an optimum commutation processwhich means that winding A is connected to the positive terminal of the inverter and windings B and C are connected to the negative terminal. Thereby, a positve and negative currents are expected to pass through windings A and B and C respectively.

Figure 7 shows the start-up torque in both cases of optimized and non-optimized commutation processes. It

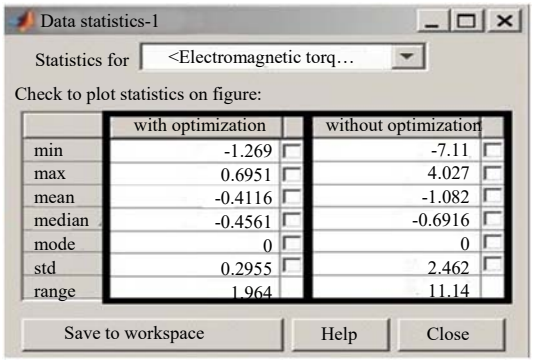

Fig. 8:

is clear the influence of optimization in reducing the start-up torque ripple, where the curve of optimized torque has a less fluctuations than the non-optimized curve

Figure 8 explores the statistical analysis for start-up torque curves, with and without optimization processes. It can be deduced that the non-optimized torque readings have larger deviations from their mean value, larger standard deviation (sd), than the readings of optimized torque curve. This statistical result, beside the resulants of Fig. 7, proves the effectiveness of the proposed method of optimized standstill commutation process in reducing the ripple of start-up torque of PM synchronous machines.

Effect of SV on the electronic commutation process: The key point of the space vector, SV, technique is to implement switching action for the electronic switching elements of the inverter at proper sequence and for proper long of period. This topic should be clearly regarded in Table 2. For instant, if the case where main and sub-domains are both 1, so the best commutation process will be achieved within the SV domain 100. Referring to Fig. 1, IGBTs 1, 5 and 6 should be fired at startup to allow to the dc bus curret to flow via winding A, A^+ and to be drained through the windings B and C, B^-C^-. The question now is how long this switching condition should continue?. The answer is related to the standard strategy of the SV technique. The PM locations 1° and 29° are both located at the same SV domain 100 but the SV technique makes a big difference in the timming period when achieving the commutation process at each of them.

CONCLUSION

A novel method has been presented in this paper to determine the best start-up commutation process. The proposed approach has proved the influence of signal injections and monitoring the corresponding impulse responses, in determining the preposition of the PM of synchronous machine at standstill condition. The validity of the approach was achieved through predicting the PM position and accordingly, determining the best configuration for machine winding excitations. The results divided the PM whole space into domains which further are divided into number of sub-domains. Consequently, the optimization of standstill commutation process for synchronous machine was specified. The work was achieved without any form of current sensors, so it characterised by high reliability, simplicity and cost effective.

REFERENCES

Assegaf, A., A. Purwadi and Y. Haroen, 2013. Dynamic response analysis of permanent magnet synchronous motor drives for city electric car. Proceedings of the International Conference on Information Technology and Electrical Engineering, October 7-8, 2013, IEEE., Yogyakarta, Indonesia, pp: 365-369.

Deshpande, Y., H.A. Toliyat and X. Wang, 2012. Standstill position estimation of SPMSM. Proceedings of the IECON 38th Annual International Conference on Industrial Electronics Society, October 25-28, 2012, IEEE., Montreal, Canada, pp: 2024-2029.

Dost, P. and C. Sourkounis, 2011. Mechanical and electrical behaviour of an electric vehicles drive train due to the choice of the control-system. Proceedings of the 37th Annual International Conference on IEEE Industrial Electronics Society, November 7-10, 2011, IEEE., Melbourne, Australia, pp: 1426-1431.

Fang, S., B. Zhou and Y. Liu, 2009. Design and realization of dual redundancy PMSM electrical drive systems. Proceedings of the 4th IEEE International Conference on Industrial Electronics and Applications, May 25-27, 2009, IEEE, Xi'an, China, pp: 1985-1989.

Iizuka, K., H. Uzuhashi, M. Kano, T. Endo and K. Mohri, 1985. Microcomputer control for sensorless brushless motor. IEEE Trans. Ind. Applic., IA-21: 595-601.

Jebai, A.K., F. Malrait, P. Martin and P. Rouchon, 2016. Sensorless position estimation and control of permanent-magnet synchronous motors using a saturation model. Int. J. Control, 89: 535-549.

Kim, H., K.K. Huh, R.D. Lorenz and T.M. Jahns, 2004. A novel method for initial rotor position estimation for IPM synchronous machine drives. IEEE. Trans. Ind. Applic., 40: 1369-1378.

Moghadam, M.A.G. and F. Tahami, 2012. Sensorless control of PMSMs with tolerance for delays and stator resistance uncertainties. IEEE. Trans. Power Electron., 28: 1391-1399.

Pillai, N.S., A.M. Vipin and R. Radhakrishnan, 2015. Analysis and simulation studies for position sensorless BLDC motor drive with initial rotor position estimation. Proceedings of the International Conference on Nascent Technologies in the Engineering Field, January 9-10, 2015, IEEE., Navi Mumbai, India, pp: 1-6.

Setty, A.R., S. Wekhande and K. Chatterjee, 2012. Comparison of high frequency signal injection techniques for rotor position estimation at low speed to standstill of PMSM. Proceedings of the IEEE 5th India Conference on Power Electronics (IICPE), December 6-8, 2012, IEEE., Delhi, India, pp: 1-6.

Wang, G., R. Yang, W. Chen, Y. Yu and D. Xu *et al*., 2009. Initial position estimation for sensorless surface-mounted PMSM with near-zero saliency at standstill. Proceedings of the IEEE International Conference on Vehicle Power and Propulsion, September 7-10, 2009, IEEE., Dearborn, Michigan, USA., pp: 1403-1406.

Yang, S.C., 2014. Saliency-based position estimation of permanent-magnet synchronous machines using square-wave voltage injection with a single current sensor. IEEE. Trans. Ind. Applic., 51: 1561-1571.

Zhang, Y., J. Gu, Z. Wu and J. Ying, 2005. Investigation of high frequency injection method for surface-mounted PMSM sensor-less drive. Proceedings of the International Conference on Electrical Machines and Systems, Volume 1, September 27-29, 2005, IEEE., Nanjing, China, pp: 306-309.

Zhaobin, H., Y. Linru and W. Zhaodong, 2014. Sensorless initial rotor position identification for non-salient permanent magnet synchronous motors based on dynamic reluctance difference. IET. Power Electron., 7: 2336-2346.